ARTICLES

Dynamics of decoherence in continuous atom-optical quantum nondemolition measurements

Roberto Onofrio[1,*] and Lorenza Viola[2]

[1]*Dipartimento di Fisica ''Galileo Galilei,'' Università di Padova, Via Marzolo 8, Padova 35131, Italy and Department of Physics and Research Laboratory of Electronics, 26-259, Massachusetts Institute of Technology, 77 Massachusetts Avenue, Cambridge, Massachusetts 02139*

[2]*d'Arbeloff Laboratory for Information Systems and Technology, Department of Mechanical Engineering, 7-040, Massachusetts Institute of Technology, 77 Massachusetts Avenue, Cambridge, Massachusetts 02139 and INFM, Sezione di Roma ''La Sapienza,'' Piazzale A. Moro 2, Roma 00185, Italy*

(Received 12 February 1998)

The Lindblad approach to continuous quantum measurements is applied to a system composed of a two-level atom interacting with a stationary quantized electromagnetic field through a dispersive coupling, fulfilling quantum nondemolition criteria. Two schemes of measurements are examined. The first one consists of measuring the atomic electric dipole, which indirectly allows one to infer the photon distribution inside the cavity. The second one schematizes a measurement of photon momentum, which permits one to describe the atomic level distribution. Decoherence of the corresponding reduced density matrices is studied in detail for both cases, and its relationship to recent experiments is finally discussed. [S1050-2947(98)04407-2]

PACS number(s): 03.65.Bz, 42.50.Ar, 42.50.Md

I. INTRODUCTION

Interaction between atoms and photons has been a fundamental issue since the early days of quantum mechanics, and it continues to be a central topic, especially in connection with controlled manipulation of small numbers of photons and atoms at the quantum level [1]. In this framework, emphasis has been placed recently on repeated measurements on atoms and photons in a quantum regime requiring that the measurement process be explicitly taken into account. It is often desirable that the outcome of a measurement is not influenced by the previous ones, which has been found to be possible by a clever choice of the measured and measuring systems. Indeed, a class of measurements aimed at repeatedly monitoring the same observable has been introduced and shown to be compatible with the foundations of quantum mechanics, the so-called quantum nondemolition (QND) measurements [2]. Many QND schemes have been proposed, and some of them have been implemented, to monitor various measurable quantities, e.g., displacements of macroscopic oscillators below the standard quantum limit [3], the photon number in traveling [4] or standing [5] electromagnetic fields, magnetic flux in superconducting interference devices [6], and the vibrational energy of an atom confined in a Paul trap [7].

From the theoretical point of view, the problem of incorporating quantum nondemolition measurements within the language of modern quantum measurement theory was not addressed specifically, to our knowledge, although important steps were taken in Refs. [8,9]. In this paper, we analyze a model for QND measurements based on Lindblad formalism, specializing it to measurement strategies aimed at describing continuous quantum nondemolition counting of photons confined in a cavity or atoms interrogated to be in a certain internal state. The system is described by a density matrix with an evolution equation introduced for generic open quantum systems [10] and already applied to other, demolitive measurement schemes such as the ones involving the quantum Zeno effect in hyperfine atomic spectroscopy [11], optogravitational cavities [12], superconducting circuits [13], and trapped ions [14]. In both cases the evolution of the coherence of the monitored system is studied, providing a simple picture of its decay during continuous QND measurements. Even starting from factorized states for atoms and photons, the measurement originates an entanglement that is ultimately responsible for the indirect decoherence of the observed system through the continuous collapse of the state of the probe. The implications of the model are discussed in connection to recent experiments implementing nondemolitive counting of photons in cavity QED [5] and atoms confined in electromagnetic traps [15].

II. QUANTUM NONDEMOLITION COUPLING AND OPEN QUANTUM SYSTEMS

A. General formalism

In this section, we recall some useful concepts related to quantum nondemolition measurements, referring the reader to Ref. [3] for a more detailed account. Although some measurements may occur through direct observation of the same observable under study, QND measurements are the most important example of indirect measurements, whereby the

*Permanent address: Dipartimento di Fisica ''G. Galilei,'' Università di Padova, Via Marzolo 8, Padova 35131, Italy. Mailing address: Department of Physics and Research Laboratory of Electronics, 26-259, Massachusetts Institute of Technology, 77 Massachusetts Ave., Cambridge, MA 02139. Electronic address: roberto@amo.mit.edu

interaction of the system S with another system P is required. The dynamics of the monitored observable $\hat{A}_S$ of the system S is inferred through the modifications induced on the actually measured observable $\hat{A}_P$ of the probe. The total Hamiltonian operator is written as

$$\hat{H}=\hat{H}_S+\hat{H}_P+\hat{H}_{\mathrm{int}}, \tag{1}$$

and the evolution of the overall system is described by the density-matrix equation

$$\frac{d}{dt}\hat{\rho}(t)=-\frac{i}{\hbar}[\hat{H}(t),\hat{\rho}(t)]. \tag{2}$$

The key idea behind a QND measurement is that the subdynamics of the observable $\hat{A}_S$ of the monitored system, albeit influencing the evolution of the probe, is not affected by this last. This nonreciprocity is obtained if the interaction Hamiltonian $\hat{H}_{\mathrm{int}}$ depends on $\hat{A}_S$ but does not commute with $\hat{A}_P$, i.e.,

$$[\hat{A}_S,\hat{H}_{\mathrm{int}}]=0, \quad [\hat{A}_P,\hat{H}_{\mathrm{int}}]\neq 0. \tag{3}$$

The subdynamics for the observables $\hat{A}_S$ and $\hat{A}_P$ are then ruled, in the Heisenberg picture, by the equations

$$i\hbar\frac{d\hat{A}_S}{dt}=[\hat{H}_S,\hat{A}_S], \quad i\hbar\frac{d\hat{A}_P}{dt}=[\hat{H}_P+\hat{H}_{\mathrm{int}},\hat{A}_P]. \tag{4}$$

In addition, the observable $\hat{A}_S$ should be protected against the evolution of all the other system observables whose subdynamics is instead unpredictably affected by the measurement, in compliance with the Heisenberg principle. This requirement restricts the class of the observables that may be monitored in a QND way, a further sufficient condition being that the observable is a constant of the motion in the absence of interaction, i.e., $[\hat{A}_S,\hat{H}_S]=0$.

This description is still not a measurement model. In particular, the unitary evolution (2) is in contrast with the general expectation that a measurement process should introduce irreversible signatures into the evolution of the system. Actually, the interaction whereby the system S is monitored by the probe P does not alone define a measurement process. As a next step, the observable $\hat{A}_P$ has to be registered and, in order that a measurement is defined univocally, this should correspond to a deterministic, classical, amount of information. It is the irreversibility implied by this act, with the pointer choosing only one of many possible quantum alternatives, that cannot be accounted for within the closed dynamics discussed so far. At the beginning of quantum theory, this problem was solved by introducing a postulate, which in the von Neumann form states the instantaneous collapse of the wave function on the eigenstate corresponding to the observed eigenvalue [16]. This approach, although applied even in recent times to various situations (including the cavity QED case as in Ref. [5]), has been overcome by a different description where a unified dynamics for quantum systems is built, without additional postulates, using the theory of open quantum systems. In this framework, the irreversible nature of the measurement is recovered by imagining the act of reading the outcome as due to an external environment which continuously interacts with the observed system. From a physical viewpoint, any process in which the interrogations on the observed system are made at a repetition rate larger than its intrinsic characteristic frequencies may be schematized as a continuous measurement. By restricting to so-called *nonselective* ensemble evolutions that can be represented in terms of a density operator, the most general dynamical law preserving (complete) positivity and normalization of the density operator was derived for a system in interaction with a Markovian environment in the form of a so-called Lindblad master equation [10], later successfully exploited in modeling quantum optics experiments [17]. Decoherence is introduced into this picture of open system evolutions as the dynamical quenching of the off-diagonal density-matrix elements, a key property first used to explain the absence of superposition states in a measurement apparatus in Ref. [18]. Within this perspective, measured systems are nothing but a special class of open quantum systems, the environment being represented by the many-mode field of the macroscopic measuring apparatus and the measurement process being equivalent to repeated instantaneous effect-valued measurements [19,20], or decoherentization kicks given to the density matrix [21]. We are thus led to the following master equation for the density of the coupled $S+P$ system undergoing a measurement through $\hat{A}_P$:

$$\frac{d}{dt}\hat{\rho}(t)=-\frac{i}{\hbar}[\hat{H}(t),\hat{\rho}(t)]-\frac{\kappa}{2}[\hat{A}_P,[\hat{A}_P,\hat{\rho}(t)]]. \tag{5}$$

The probe observable $\hat{A}_P$ plays the role of a Lindblad operator representing the influence of the external environment, and the parameter κ, with dimensions $[\kappa]=[t^{-1}A^{-2}]$, gives the coupling (generally time dependent) of the probe to the measurement apparatus. By choosing a continuous function of time $\kappa(t)$, a continuous measurement process is obtained.

B. Atom-photon Hamiltonian

In the following, we will discuss quantum nondemolition counting schemes for both photons confined in a cavity and two-level atoms in a given eigenstate. By denoting with $\hat{a}$ and $\hat{a}^\dagger$ the standard annihilation and creation bosonic operators, the Hamiltonian of the free single-mode electromagnetic field is written as

$$\hat{H}_{\mathrm{photon}}=\hbar\omega\hat{a}^\dagger\hat{a}, \tag{6}$$

while the two-level Hamiltonian can be expressed as

$$\hat{H}_{\mathrm{atom}}=\hbar\omega_{ef}\hat{\sigma}_z \tag{7}$$

with respect to the basis of the energy eigenstates $|e\rangle,|f\rangle$, $\omega_{ef}=(E_e-E_f)/\hbar$. It is convenient to shift the zero of energy in order to have $E_f=0$, which is equivalent to choose the following shifted two-level Hamiltonian

$$\hat{H}_{\mathrm{atom}}=\hbar\omega_{ef}\left(\frac{\hat{I}}{2}+\hat{\sigma}_z\right)=\hbar\omega_{ef}\hat{\sigma}_+\hat{\sigma}_-=\hbar\omega_{ef}\hat{\Pi}_e, \tag{8}$$

where $\hat{\sigma}_+$, $\hat{\sigma}_-$ and $\hat{\Pi}_e = \hat{\sigma}_+ \hat{\sigma}_-$ denote the Pauli displacement operators and the projector over the excited state $|e\rangle$, respectively. Based on the previous considerations, we choose an interaction Hamiltonian which is linear in both the photon number operator $\hat{a}^\dagger \hat{a}$ and the atomic projector $\hat{\Pi}_e$,

$$\hat{H}_{int} = 2\hbar\gamma \hat{a}^\dagger \hat{a} \hat{\Pi}_e, \tag{9}$$

the coefficient 2γ, a measurement angular frequency, quantifying the strength of the quantum nondemolition coupling. The occupation probability of level $|e\rangle$ for an atom in a generic state $\hat{\rho}^{(\text{atom})}$ is $P_e = \text{Tr}\{\hat{\rho}^{(\text{atom})} \hat{\Pi}_e\}$. We note that, provided the Hamiltonian (8) is reinterpreted as a single-particle operator for an ensemble of independent atoms, and collective effects due to quantum statistics or interatomic forces are neglected, the probability P_e is related directly to the average number n_e of atoms in level $|e\rangle$ through $n_e = P_e n_T$, n_T being the total number of atoms. Once chosen as the system observable $\hat{A}_S$, both the photon number operator and the atomic occupation probability automatically satisfy the commutation relationship with the respective Hamiltonians (6) and (8) since, in the absence of interactions, they are conserved. The total Hamiltonian to be used in Eq. (5) is written explicitly as

$$\hat{H} = \hbar\omega \hat{a}^\dagger \hat{a} + \hbar\omega_{ef} \hat{\sigma}_+ \hat{\sigma}_- + 2\hbar\gamma \hat{a}^\dagger \hat{a} \hat{\sigma}_+ \hat{\sigma}_-. \tag{10}$$

We will be working in the representation of the unperturbed (field plus atom) eigenstates, expanding the density operator as

$$\hat{\rho}(t) = \sum_{a,b=e,f} \sum_{n,m=0}^{\infty} \rho_{an,bm}(t) |an\rangle\langle bm|, \tag{11}$$

where $\rho_{an,bm}(t) = \langle an|\hat{\rho}(t)|bm\rangle$. It may be worth looking, for a moment, at the closed evolution of the density-matrix elements. By projecting Eq. (2) [or Eq. (5) with $\kappa = 0$], we find

$$\begin{aligned} \dot{\rho}_{fn,fm} &= -i\omega(n-m)\rho_{fn,fm}, \\ \dot{\rho}_{en,em} &= -i(\omega+2\gamma)(n-m)\rho_{en,em}, \\ \dot{\rho}_{fn,em} &= -i[\omega(n-m) - \omega_{ef} - 2\gamma m]\rho_{fn,em}, \end{aligned} \tag{12}$$

whose solutions are simply rotations of the initial density-matrix elements

$$\begin{aligned} \rho_{fn,fm}(t) &= \exp[-i\omega(n-m)t]\rho_{fn,fm}(0), \\ \rho_{en,em}(t) &= \exp[-i(\omega+2\gamma)(n-m)t]\rho_{en,em}(0), \\ \rho_{fn,em}(t) &= \exp\{-i[\omega(n-m) - \omega_{ef} - 2\gamma m]t\}\rho_{fn,em}(0), \end{aligned} \tag{13}$$

and $\rho_{en,fm}(t) = \rho^*_{fm,en}(t)$. These equations imply obviously that both the average photon number and the average occupation probabilities of level $|e\rangle$ are time independent, consistent with the QND nature of the interaction. On the other hand, the photon-atom interaction induces additional phase shifts in the density matrix, which are proportional to the strength of the coupling γ and depend upon the atomic and the photonic state. These phase shifts contain the useful information about the system that needs to be extracted through the measurement on the probe. In Secs. III and IV, we will examine two complementary measurement procedures based on this optoatomic coupling.

III. QND ELECTROMAGNETIC FIELD MEASUREMENTS VIA ATOMIC DIPOLE QUADRATURE

A first class of QND measurements in optoatomic systems is obtained by monitoring the photon field using nonresonant atoms as the probe system. This corresponds to

$$\hat{H}_S = \hat{H}_{\text{photon}}, \quad \hat{H}_P = \hat{H}_{\text{atom}}, \quad \hat{A}_S = \hat{a}^\dagger \hat{a}. \tag{14}$$

Accordingly, Hamiltonian (10) represents the fact that the photons in the cavity induce a state-dependent dynamical Stark effect on the atom and a selective phase shift of the atomic wave function. Due to the requirement of noncommutativity between the probe observable and the interaction Hamiltonian, we discard any operator proportional to the Pauli matrix $\hat{\sigma}_z$ as an atomic probe operator $\hat{A}_P$. On the other hand, in order to model a measurement which is sensitive to the dephasing accumulated between the components e and f of the atom interacting with the mode, phase-sensitive observables like the quadrature components of the atomic dipole operator $\hat{\sigma}_y = (\hat{\sigma}_+ - \hat{\sigma}_-)/2i$, are natural candidates. Indeed, we observe that for a proper atomic superposition state, $|\psi\rangle = a|e\rangle + b|f\rangle$, $a = |a|\exp(i\phi_a)$, $b = |b|\exp(i\phi_b)$, $|a|,|b| \neq 0$, and the average value $\langle\sigma_y\rangle = |a||b|\sin(\phi_a - \phi_b)$ is nonzero whenever a relative phase $(\phi_a - \phi_b)$ is present. By comparison, $\langle\sigma\rangle_x = |a||b|\cos(\phi_a - \phi_b)$, maintaining finite values even if the relative phase, vanishes. We therefore choose

$$\hat{A}_P = \frac{\hat{\sigma}_+ - \hat{\sigma}_-}{2i} \tag{15}$$

as the probe observable, and by using Eq. (5) we obtain the following equations of motion:

$$\begin{aligned} \dot{\rho}_{fn,fm} &= -i\omega(n-m)\rho_{fn,fm} - \frac{\kappa}{4}(\rho_{fn,fm} - \rho_{en,em}), \\ \dot{\rho}_{en,em} &= -i(\omega+2\gamma)(n-m)\rho_{en,em} - \frac{\kappa}{4}(\rho_{en,em} - \rho_{fn,fm}), \\ \dot{\rho}_{fn,em} &= -i[\omega(n-m) - \omega_{ef} - 2\gamma m]\rho_{fn,em} \\ &\quad - \frac{\kappa}{4}(\rho_{fn,em} + \rho_{en,fm}), \end{aligned} \tag{16}$$

$\dot{\rho}_{en,fm} = \dot{\rho}^*_{fm,en}$. We note that the evolutions for atomic diagonal and nondiagonal entries are decoupled but, at variance with the situations analyzed in Refs. [11–14], the measurement affects all components.

By introducing the two families of pseudofrequencies u and w, defined as

$$u(n,m)=\sqrt{\gamma^2(n-m)^2-\frac{\kappa^2}{16}},\quad w(n,m)=\sqrt{[\omega_{ef}+\gamma(n+m)]^2-\frac{\kappa^2}{16}}, \tag{17}$$

Eqs. (16) are exactly solved, giving

$$\begin{aligned}\rho_{fn,fm}(t)&=e^{-i(n-m)(\omega+\gamma)t-\kappa t/4}\left\{\left[\cos ut+i(n-m)\gamma\frac{\sin ut}{u}\right]\rho_{fn,fm}(0)+\frac{\kappa}{4}\frac{\sin ut}{u}\rho_{en,em}(0)\right\},\\ \rho_{en,em}(t)&=e^{-i(n-m)(\omega+\gamma)t-\kappa t/4}\left\{\left[\cos ut-i(n-m)\gamma\frac{\sin ut}{u}\right]\rho_{en,em}(0)+\frac{\kappa}{4}\frac{\sin ut}{u}\rho_{fn,fm}(0)\right\},\\ \rho_{fn,em}(t)&=e^{-i(n-m)(\omega+\gamma)t-\kappa t/4}\left\{\left[\cos wt+i[\omega_{ef}+(n+m)\gamma]\frac{\sin wt}{w}\right]\rho_{fn,em}(0)-\frac{\kappa}{4}\frac{\sin wt}{w}\rho_{en,fm}(0)\right\},\end{aligned} \tag{18}$$

where the dependence of frequencies u and w on photon numbers n and m is understood. As expected, Eqs. (18) reduce to Eq. (13) when no measurement is performed, $\kappa=0$, and for open-system coupling κ small compared to γ, the dynamics of the coupled $S+P$ system is just weakly perturbed with respect to the closed case. In the opposite regime, where $\kappa\gg\gamma$ and a proper measurement on the signal mode is performed, pseudofrequencies u and w tend to become purely imaginary, introducing overdamped oscillations and thereby decoherence. The time development of the electromagnetic field under the effect of the measurement can be inspected by evaluating the reduced density matrix:

$$\begin{aligned}\rho_{nm}^{(\text{field})}(t)=\sum_{a=e,f}\rho_{an,am}(t)=e^{-i(n-m)(\omega+\gamma)t-\kappa t/4}&\left\{\left[\cos ut+\left(i(n-m)\gamma+\frac{\kappa}{4}\right)\frac{\sin ut}{u}\right]\rho_{ff}^{(\text{atom})}(0)\right.\\ &\left.+\left[\cos ut+\left(-i(n-m)\gamma+\frac{\kappa}{4}\right)\frac{\sin ut}{u}\right]\rho_{ee}^{(\text{atom})}(0)\right\}\rho_{nm}^{(\text{field})}(0),\end{aligned} \tag{19}$$

where an initially uncorrelated state $\rho_{an,bm}(0)=\rho_{ab}^{(\text{atom})}(0)\rho_{nm}^{(\text{field})}(0)$ has been assumed. It is immediate to recognize that, for every κ, field populations are unaffected by the measurement, i.e., $\rho_{nn}^{(\text{field})}(t)=\rho_{nn}^{(\text{field})}(0)$, in agreement with the QND nature of the coupling. However, the process of acquiring information on the field photon number cannot be realized without a back-action on the conjugate field variable, specifically an unavoidable degradation of the field phase distribution. A direct visualization of the phase evolution is provided by suitable phase-coherence indicators. Here we adopt the formalism of the so-called Pegg-Barnett phase distribution discussed at length in Ref. [22]:

$$\Pi^{PB}(\theta,t)=\lim_{s\to\infty}\frac{1}{2\pi}\sum_{n,m=0}^{s}\rho_{nm}^{(\text{field})}(t)e^{-i(n-m)\theta}. \tag{20}$$

We have analyzed in detail the evolution arising when the field is initially in a coherent state $|\alpha e^{i\phi}\rangle$ with a mean photon number α^2, and the probe state is an equal superposition of levels e,f. As it will become clear in Sec. V, these choices will enable us a straightforward comparison with the results reported in Ref. [5]. We note, however, that equivalent physical insight would be gained from using a different standard quantum-optical distribution, the so-called Q function [23]. Starting as a sharply peaked function centered at $\theta=\phi$, the Pegg-Barnett distribution retains its form when $\gamma=0$, the only changes reflecting the rotation of the coherent state in phase space. When $\gamma\neq 0$ but $\kappa=0$, the phase distribution is split into two components moving at different velocities with relative weights proportional to the coefficients of the atomic wave function. The evolution is strikingly different in the presence of measurement, since the phase distribution is progressively scrambled until it becomes completely flat when field coherences are asymptotically destroyed, $\rho_{nm}^{(\text{field})}(t)\to 0$, $n\neq m$. The probability distribution (20) is shown in Fig. 1 for various instants of time and two different values of κ corresponding to small and strong coupling with the environment. In the case of weak coupling (solid line), the splitting of the initial, well-defined phase distribution, into two components traveling with different velocities is still recognizable.

IV. QND ATOMIC MEASUREMENTS VIA PHOTON MOMENTUM

A second class of QND measurements is obtained if, according to the notations of Sec. II A, we choose

$$\hat{H}_S=\hat{H}_{\text{atom}},\quad \hat{H}_P=\hat{H}_{\text{photon}},\quad \hat{A}_S=\hat{\Pi}_e. \tag{21}$$

This corresponds to monitoring the atomic level via an electromagnetic field, and is realized ordinarily by means of an absorption process, i.e., by sending photons resonantly tuned at an energy-level gap. This technique is manifestly demolitive for the interrogated atoms. An alternative approach consists in the detection of the phase-shift originated by the atom through a nonresonant interaction with a light beam, the atomic sample acting as a dispersive medium with a complex refraction index. A nice application of this technique was recently reported in Ref. [15], where repeated, nondestructive optical imaging of an atomic cloud confined

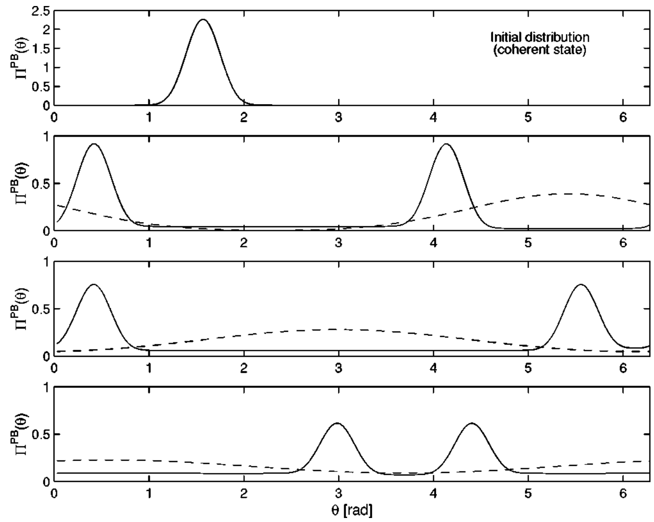

FIG. 1. Time evolution of the Pegg-Barnett phase distribution for a coherent state of the electromagnetic field and various values of the measurement coupling constant $\kappa = 10^{-1}$ (solid line) and 10 (dashed line) in the continuous case. The first 20 energy eigenstates have been used as a truncated basis for the photon field, leading to a numerical accuracy of 0.1%. The snapshots from above to below are taken at times differing by one measurement period defined as $T_m = 2\pi/2\gamma$.

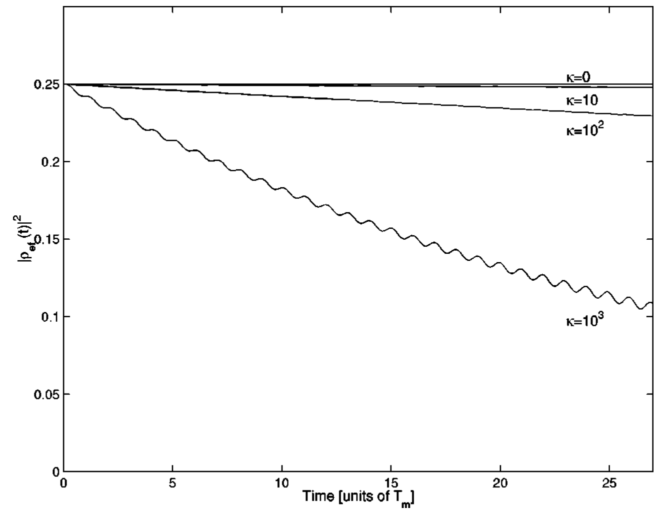

FIG. 2. Square modulus of the atomic reduced density matrix $|\rho_{ef}|^2$ vs time (in units of the measurement period T_m) for various values of κ. The oscillations are also present in the closed case $(\kappa = 0)$, although not visible in the scale, and corresponds to the behavior of Eq. (25).

in a magnetic trap was demonstrated. The modification of the refraction index, proportional to the atomic optical density, induces a phase shift of the probe field which is manifested in turn as a change in the amplitude of its quadrature component. The dispersive phase shifts may be also detected through amplitude modulation by means of classical, standard techniques like dark-ground or phase-contrast imaging [15]. In our model, it is natural to choose the following phase-sensitive photon operator

$$\hat{A}_P = \frac{\hat{a}^\dagger - \hat{a}}{2i} \tag{22}$$

as a probe observable. This choice, in addition to fulfilling the QND criteria established above, corresponds to a measurement configuration which is the dual of the one analyzed in Sec. IV. By exploiting the master equation (5) again, and by evaluating the new Lindblad commutator, equations of motion of the following form are derived:

$$\begin{aligned}\dot{\rho}_{an,bm} = \dot{\rho}^{(\kappa=0)}_{an,bm} - \frac{\kappa}{4}\Big[&(n+m+1)\rho_{an,bm} \\ &+ \sqrt{n(m+1)}\rho_{an-1,bm+1} + \sqrt{m(n+1)}\rho_{an+1,bm-1} \\ &- \sqrt{nm}\rho_{an-1,bm-1} - \sqrt{(n+1)(m+1)}\rho_{an+1,bm+1} \\ &- \frac{1}{2}\Big(\sqrt{n(n-1)}\rho_{an-2,bm} + \sqrt{m(m-1)}\rho_{an,bm-2} \\ &+ \sqrt{(n+1)(n+2)}\rho_{an+2,bm} \\ &+ \sqrt{(m+1)(m+2)}\rho_{an,bm+2}\Big)\Big],\end{aligned} \tag{23}$$

where $a,b = e,f$ and $n,m \geqslant 0$, and $\dot{\rho}^{(\kappa=0)}_{an,bm}$ indicates, for brevity, the appropriate unmeasured contribution, shown explicitly in Eqs. (12). Since, as before, the probe observable $\hat{A}_P$ is diagonal in the system variables, no transitions are induced by the measurement process in the system. In this case, the e and f components evolve independently, but a quite complicated structure of the couplings in the Fock space of the photons is present in general. Equations (23) have been integrated numerically for a field coherent state and an equal-weight atomic superposition state. The reduced density matrix that is appropriate to study the evolution of the signal mode during the measurement is the atomic density obtained by tracing the total density matrix over the photonic degrees of freedom,

$$\rho^{(atom)}_{ab}(t) = \sum_{n=0}^{\infty} \rho_{an,bn}(t). \tag{24}$$

By analogy with the previous case, we expect that although no perturbation is introduced on the variable which is QND monitored, i.e., $\rho^{(\mathrm{atom})}_{ee}(t) = \rho^{(\mathrm{atom})}_{ee}(0)$, atomic coherence is eroded due to back-action. In Fig. 2, the time dependence of the coherence indicator $|\rho_{ef}(t)|$ is plotted for different values of the coupling parameter κ. The evolution of atomic coherence in the closed case $\kappa = 0$ can be evaluated explicitly for a coherent probe state since, from Eqs. (12),

$$\begin{aligned}\rho_{ef}(t) &= \tfrac{1}{2}\, e^{i\omega_{ef}t} \sum_{n=0}^{\infty} e^{2i\gamma nt} \rho^{(\mathrm{field})}_{nn}(0) \\ &= \tfrac{1}{2}\, e^{\alpha^2(\cos 2\gamma t - 1)}\, e^{i(\omega_{ef}t + \alpha^2 \sin 2\gamma t)}.\end{aligned} \tag{25}$$

This shows that the quantity $|\rho_{ef}(t)|^2$ oscillates with angular frequency 2γ between a maximum value equal to $\frac{1}{4}$ and a strictly positive minimum equal to $e^{-4\alpha^2}/4$, leading to an example of nontrivial reversible dynamics of the modulus of the atomic coherence. In the presence of measurement, atomic coherence damps exponentially to zero with a rate proportional to the parameter κ, still preserving the oscillatory behavior visible in Fig. 2.

V. EXPERIMENTAL COMPARISON

The model developed here, describing decoherence induced by a continuous QND measurement, is characterized completely by the parameters γ and κ. In this section we discuss to what extent these parameters can be related to a realistic experimental scheme. The example we take is the scheme proposed and implemented by a group at the Ecole Normale Supérieure [5], where atoms detect in a nondemolitive way the photons stored in a high-Q cavity. In their scheme, the atom is schematized as a system with three Rydberg levels e, f, and i, with levels i and f of the same parity, opposite to the one of level e. The frequency ω of the cavity mode is detuned from the $e \rightarrow i$ transition by an amount $\delta = \omega - |\omega_{ie}|$. The detuning is large enough to neglect photon absorption, but small in comparison to the angular frequency ω_{ie}. The presence of photons in the cavity results in a phase-shift of the e state relative to the f state. We recall that the dynamical frequency shift induced on an atom in level e and atomic dipole d and located at point r in a cavity containing N photons is

$$\Delta_e(r,N) = \frac{\delta}{2}\left\{\left[1 + \frac{4E(r)^2 d^2}{\hbar^2 \delta^2} N\right]^{1/2} - 1\right\} \simeq \frac{E(r)^2 d^2}{\hbar^2 \delta} N = \frac{\Omega(r)^2}{\delta} N, \tag{26}$$

where $E(r)$ is the electric field at r and the last approximation holds if absorption processes are made negligible. The phase shift is proportional to the vacuum Rabi angular frequency $\Omega(r) = E(r)d/\hbar$. Noticing that N is the eigenvalue of the $\hat{a}^\dagger \hat{a}$ operator, we can think of the spatially averaged phase shift as due to the effective Hamiltonian

$$\hat{H}_{int} = \hbar \frac{\langle \Omega^2(r) \rangle}{\delta} \hat{a}^\dagger \hat{a} \hat{\Pi}_e . \tag{27}$$

The parameter γ of our model is therefore identified as $\gamma = \langle \Omega^2(r) \rangle / 2\delta$. Concerning the parameter κ, the discussion is more elaborate, since in the realistic situation analyzed in Ref. [5] the measuring meter is actually a beam of two-level atoms crossing the cavity and the effect of the measurement is taken into account using the von Neumann collapse for each atomic interaction. Distinction is made between two different configurations of the probe system, corresponding to either atoms with a known initial velocity that are registered by the field ionization counters, or atoms which are not in a monokinetic velocity state and are not read. In the language of quantum measurement theory, this difference can be restated in terms of *selective* and *nonselective* measurements [11], nonselective dynamics being obtained by averaging over all the possible states of the probe, in this case over the velocity distribution measurements and the two possible outcomes of the internal level. To make an explicit comparison with Ref. [5], it was shown there that the selective evolution of the field density matrix at the $(k+1)$th atomic detection event is given by

$$\rho_{nm}^{(k+1)}(a,v) = \frac{b_a(n,v) b_a^*(m,v)}{\sum_n |b_a(n,v)|^2} \rho_{nm}^{(k)}(a,v), \tag{28}$$

where $b_a(n,v)$ denotes the amplitude of the component a $(a=e,f)$ corresponding to a generic atomic velocity v and a photon number n. As first step toward nonselective measurements, we need to evaluate the weighted average over the possible final outcome of the probe, leading to

$$\rho_{nm}^{(k+1)}(v) = \sum_{a=e,f} b_a(n,v) b_a^*(m,v) \rho_{nm}^{(k)}(v) = \left\{ \sin^2 \frac{\pi v_0}{4v} + \cos^2 \frac{\pi v_0}{4v} e^{-i\epsilon(n-m)v_0/v} \right\} \rho_{nm}^{(k)}(v), \tag{29}$$

where the parameter ϵ measures the accumulated phase shift per photon, and v_0 is the atomic velocity corresponding to a $\pi/2$ pulse in the Ramsey zone used for interferometric detection of the dephasing. The next step is a second integration over the atomic velocity distribution $P(v)$:

$$\rho_{nm}^{(k+1)} = \int dv \; P(v) \sum_{a=e,f} b_a(n,v) b_a^*(m,v) \rho_{nm}^{(k)}(v). \tag{30}$$

In Figs. 3 and 4, the Pegg-Barnett phase distribution is plotted for a monokinetic atomic beam [Eq. (29)] and a thermal atomic beam [Eq. (30)], respectively. While in both situations the phase distribution is broadened and tends towards a flat behavior, only in the second case does the transient resemble the behavior found for a nonselective measurement by using the effective Lindblad approach, cf. Fig. 1. In particular, the velocity of the decoherence is proportional to the temperature of the atomic beam, i.e., the beam variance. This qualitatively agrees with the result established in Ref. [11], concerning the direct proportionality between the measurement coupling constant and the temperature of the bath in which the meter is embedded [11]. Unlike the parameter γ, it is not possible to infer a simple relationship relating κ to the various parameters of the realistic configuration. This shows the advantages and disadvantages of the effective Lindblad approach: it is often impossible to relate it completely with the experimental setup; however, a general description of

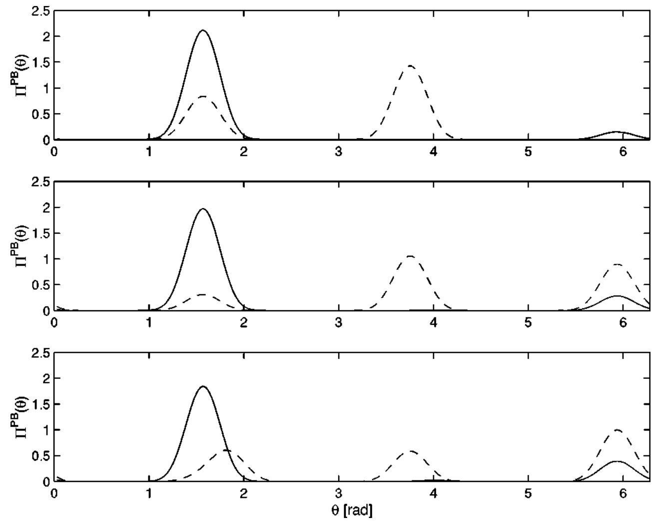

FIG. 3. Time evolution of the Pegg-Barnett phase distribution for a Von Neumann measurement on a coherent state of the electromagnetic field (with initial Pegg-Barnett phase distribution as in Fig. 1), corresponding to consecutive interrogations with a monokinetic beam at two different velocities, $v/v_0=0.3$ (solid) and $v/v_0=0.6$ (dashed). The phase is progressively scrambled, although its spreading starts from well-defined regions.

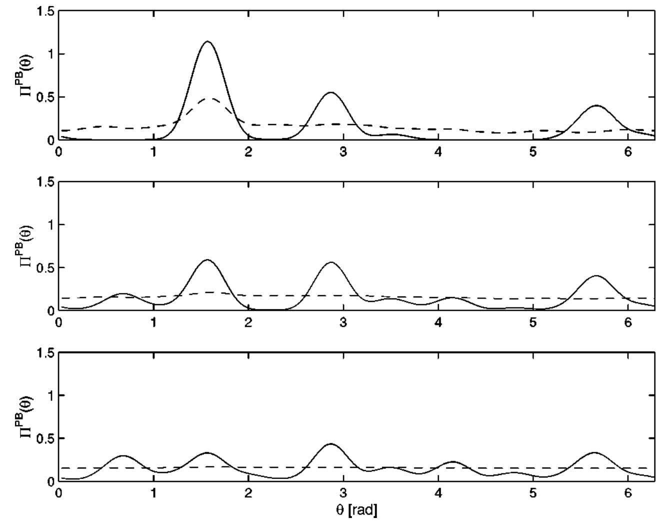

FIG. 4. Time evolution of the Pegg-Barnett phase distribution for a Von Neumann measurement on a coherent state of the electromagnetic field (with initial Pegg-Barnett phase distribution as in Fig. 1) with thermal atoms for two different temperatures (in arbitrary units) $T=10^{-1}$ (solid line) and $T=10$ (dashed line). The scrambling of the phase is faster than in the monokinetic case, affecting all the phases, and is proportional to the temperature.

any measurement process is obtained without a detailed knowledge of the actual experimental procedure. For this reason, the formalism may be easily adapted to the description of other relevant schemes, like the single photon-atom coupling in a high-finesse Fabry-Perot cavity [24], the QND counting of atoms in an optogravitational cavity based upon use of evanescent fields [25,26], and the nondestructive imaging of a Bose-Einstein atomic condensate [15]. For the latter system, the dephasing of the atomic coherence induced by the measurement process should generate damping of the oscillatory behavior of either a two-species condensate exhibiting Rabi-like oscillations, or two single-component condensates spatially separated and undergoing coherent, Josephson-like oscillations—a situation similar to the one involving a superconducting circuit already analyzed in Ref. [13].

VI. CONCLUSIONS

A model for the description of the decay of coherence in continuous quantum nondemolition measurements involving photons and atoms has been developed and applied to photon and atom counting. Even if initially uncorrelated, atoms and photons become entangled during the measurement and, although conserving their number, they are subjected to decoherence due to the back-action via the probe. The dynamics of the system has been analytically solved in the case of photon counting via atomic detection. The decay of atomic coherence has been proven when the atomic occupation probability is measured through the monitoring of the light beam. Contact has been established with actual experiments in which decoherence induced by the measurement process is or could be observable. In particular, the nondestructive monitoring of Bose-Einstein condensates of atomic dilute gas through dispersive imaging, demonstrated in Ref. [15], will deserve a particular attention, since the influence of the measurement on the dynamics of the phase of the wave function is a crucial issue in the study of macroscopic quantum coherence. More in general, this model gives constraints on the minimum rate at which coherence is progressively destroyed during a continuous measurement process even if a quantum nondemolition monitoring is adopted, provided that all other possible sources of decoherence have been quenched by proper technological improvements. As a consequence, similar considerations should also be relevant to investigate decoherence dynamics within QED-based quantum computation proposals [27,28] or quantum control strategies involving QND-mediated feedback [29]. Finally, we point out that, in the model described here, emphasis has been put on considering the whole coupled (system plus probe) object as an open quantum system in interaction with a measuring environment, the probe degrees of freedom being traced out on the total density matrix and not dynamically eliminated from the beginning. This makes the description formally different from other existing approaches [8,9]. A quantitative discussion of the equivalence between the two strategies will be addressed elsewhere [30].

ACKNOWLEDGMENTS

We are grateful to Wolfgang Ketterle and Chandra S. Raman for a critical reading of the manuscript. Use of computing facilities of the INFN, Sezione di Padova, and MIT is acknowledged. R.O. was supported by the CNR, Italy, through the NATO Advanced Fellowships Program, and MURST, Italy. L.V. was supported by the University of Padova and wishes to acknowledge the MIT Department of Physics for its hospitality during the period this work began.

[1] For a general overview, see, for instance, C. Cohen-Tannoudji, J. Dupont-Roc, and G. Grynberg, *Atom-Photon Interactions: Basic Processes and Applications* (Wiley, New York, 1992).

[2] V. B. Braginsky and F. Ya. Khalili, in *Quantum Measurements*, edited by K. S. Thorne (Cambridge University Press, Cambridge, 1992).

[3] C. M. Caves, K. S. Thorne, R. P. Drever, V. D. Sandberg, and M. Zimmermann, Rev. Mod. Phys. **52**, 341 (1980); M. F. Bocko and R. Onofrio, *ibid.* **68**, 755 (1996).

[4] M. D. Levenson, R. M. Shelby, M. Reid, and D. F. Walls, Phys. Rev. Lett. **57**, 2473 (1986); N. Imoto, S. Watkins, and Y. Sasaki, Opt. Commun. **61**, 159 (1987); A. LaPorta, R. E. Slusher, and B. Yurke, Phys. Rev. Lett. **62**, 28 (1989); P. Grangier, J. F. Roch, and G. Roger, *ibid.* **66**, 1418 (1991); J.-F. Roch, K. Vigneron, Ph. Grelu, A. Sinatra, J.-Ph. Poizat, and P. Grangier, *ibid.* **78**, 634 (1997).

[5] M. Brune, S. Haroche, V. Lefevre, J. M. Ramond, and N. Zagury, Phys. Rev. Lett. **65**, 976 (1990); M. Brune, S. Haroche, J. M. Ramond, L. Davidovich, and N. Zagury, Phys. Rev. A **45**, 5193 (1992); L. Davidovich, M. Brune, J. M. Ramond, and S. Haroche, *ibid.* **53**, 1295 (1996).

[6] T. Calarco and R. Onofrio, Phys. Lett. A **198**, 279 (1995).

[7] R. L. de Matos Filho and W. Vogel, Phys. Rev. Lett. **76**, 4520 (1996).

[8] G. J. Milburn and D. F. Walls, Phys. Rev. A **28**, 2065 (1983).

[9] M. J. Gagen and G. J. Milburn, Phys. Rev. A **45**, 5228 (1992); G. J. Milburn and M. J. Gagen, Phys. Rev. A **46**, 1578 (1992).

[10] G. Lindblad, Commun. Math. Phys. **48**, 119 (1976); V. Gorini, A. Kossakowsky, and E. C. G. Sudarshan, J. Math. Phys. **17**, 821 (1976).

[11] C. Presilla, R. Onofrio, and U. Tambini, Ann. Phys. (N.Y.) **248**, 95 (1996).

[12] R. Onofrio and L. Viola, Phys. Rev. A **53**, 3773 (1996).

[13] L. Viola, R. Onofrio, and T. Calarco, Phys. Lett. A **229**, 23 (1997).

[14] L. Viola and R. Onofrio, Phys. Rev. A **55**, R3291 (1997).

[15] M. R. Andrews, M.-O. Mewes, N. J. van Druten, D. S. Durfee, D. M. Kurn, and W. Ketterle, Science **273**, 84 (1996).

[16] J. von Neumann, *Die Mathematischen Grundlagen der Quantenmechanik* (Springer, Berlin, 1932).

[17] J. Carmichael, *An Open Systems Approach to Quantum Optics* (Springer-Verlag, Berlin, 1993).

[18] W. H. Zurek, Phys. Rev. D **24**, 1516 (1981); **26**, 1862 (1982).

[19] A. Barchielli, L. Lanz, and G. M. Prosperi, Nuovo Cimento B **72**, 121 (1982).

[20] C. M. Caves and G. J. Milburn, Phys. Rev. A **36**, 5543 (1987).

[21] The density-matrix formalism is not the only available language to depict open-system evolutions. So-called *selective* descriptions based upon stochastic differential equations or quantum trajectories have been also introduced; see, for instance, N. Gisin, Phys. Rev. Lett. **52**, 1657 (1984); L. Diosi, N. Gisin, J. Halliwell, and I. C. Percival, *ibid.* **74**, 203 (1995). Decoherence can be more properly modeled as a phase-diffusion process in those contexts.

[22] D. T. Pegg and S. M. Barnett, Phys. Rev. A **39**, 1665 (1989); S. M. Barnett and D. T. Pegg, *ibid.* **41**, 3427 (1990).

[23] M. J. Werner and H. Risken, Quantum Opt. **3**, 185 (1991); V. Bužek, H. Moya-Cessa, P. L. Knight, and S. J. D. Phoenix, Phys. Rev. A **45**, 8190 (1992).

[24] H. J. Kimble, in *Cavity Quantum Electrodynamics*, edited by P. R. Berman (Academic, San Diego, 1994); K. An, J. J. Childs, R. R. Dasari, and M. S. Feld, Phys. Rev. Lett. **73**, 3375 (1994).

[25] J.-Y. Courtois, J.-M. Courty, and S. Reynaud, Phys. Rev. A **52**, 1507 (1995).

[26] A. Aspect, R. Kaiser, N. Vansteenkiste, P. Vignolo, and C. I. Westbrook, Phys. Rev. A **52**, 4704 (1995).

[27] J. M. Raimond, M. Brune, and S. Haroche, Phys. Rev. Lett. **79**, 1964 (1997).

[28] T. Pellizzari, S. A. Gardiner, J. I. Cirac, and P. Zoller, Phys. Rev. Lett. **75**, 3788 (1995); E. Knill and R. Laflamme, Phys. Rev. A **55**, 900 (1997).

[29] P. Tombesi and D. Vitali, Phys. Rev. A **50**, 4253 (1994); D. Vitali, P. Tombesi, and G. J. Milburn, Phys. Rev. Lett. **79**, 2442 (1997).

[30] L. Viola (unpublished).